Physics in Medicine & Biology

IPEM Institute of Physics and Engineering in Medicine

PAPER • OPEN ACCESS

# *In situ* correction of recombination effects in ultra-high dose rate irradiations with protons

To cite this article: R Schaefer *et al* 2023 *Phys. Med. Biol.* **68** 105013

IOP Publishing Phys. Med. Biol. 68 (2023) 105013 https://doi.org/10.1088/1361-6560/accf5c

Physics in Medicine & Biology

IPEM Institute of Physics and Engineering in Medicine

OPEN ACCESS

RECEIVED
6 January 2023

REVISED
15 March 2023

ACCEPTED FOR PUBLICATION
21 April 2023

PUBLISHED
11 May 2023



PAPER

# *In situ* correction of recombination effects in ultra-high dose rate irradiations with protons

**R Schaefer**[1,*], **S Psoroulas**[1] **and D C Weber**[1,2,3]

[1] Centre for Proton Therapy, Paul-Scherrer-Institute (PSI), Villigen, Switzerland
[2] Department of Radiation Oncology, University Hospital Zurich, Zurich, Switzerland
[3] Department of Radiation Oncology, Inselspital, Bern University Hospital, University of Bern, Switzerland
[*] Author to whom correspondence should be addressed.

**E-mail:** robert.schaefer@psi.ch

**Keywords:** recombination effects, ultra-high dose rates, gas-based ionization chamber, FLASH, proton beams

## Abstract

*Background.* At the Center for Proton Therapy at the Paul Scherrer Institute (PSI) the delivery of proton radiation is controlled via gas-based ionization chambers: the beam is turned off when a certain amount of preset charge has been collected. At low dose rates the charge collection efficiency in these detectors is unity, at ultra-high dose rates it is less due to induced charge recombination effects. If not corrected, the latter would lead to an overdosage. *Purpose.* In the scope of this work, we developed a novel approach to an *in situ* charge recombination correction for our dose defining detectors, when irradiated with a proton beam at ultra-high dose rates. This approach is based on the Two-Voltage-Method. *Methods.* We have translated this method to two separate devices operated simultaneously at different conditions. By doing so, the charge collection losses can be corrected directly and without the need for empirical correction values. This approach has been tested at ultra-high dose rates; proton beam was delivered by the COMET cyclotron to Gantry 1 at PSI. *Results.* We were able to correct the charge losses caused by recombination effects at local beam currents of approximately 700 nA (i.e. instantaneous dose rate of 3600 Gy $s^{-1}$ at isocenter). The corrected collected charges in our gaseous detectors were compared against recombination-free measurements with a Faraday cup. The ratio of both quantities shows no significant dose rate dependence within their respective combined uncertainties. *Conclusions*. Correcting recombination effects in our gas-based detectors with the novel method greatly eases the handling of Gantry 1 as 'FLASH test bench'. Not only is the application of a preset dose more accurate compared to using an empirical correction curve, also the re-determination of empirical correction curves in the case of a beam phase space change can be omitted.

## 1. Introduction

With the re-discovery and the demonstration of the preclinical FLASH effect (Favaudon *et al* 2014, Vozenin *et al* 2019) with electron beams, clinical proton units have been adapted for ultra-high dose rate (UHDR) conditions, and in some cases have been even used for first demonstrations of the FLASH effect in mice (Diffenderfer *et al* 2020, Cunningham *et al* 2021, Singers Sørensen *et al* 2022) and Zebrafish embryos (Beyreuther *et al* 2019). Even though the mechanism of the FLASH effect has not yet been fully understood, and results of studies investigating the FLASH effect with proton beams sometimes have been non-consistent (Wilson *et al* 2019), the need for facilities capable of delivering proton beams with dose rates over several orders of magnitude higher compared to clinical dose rates remains to allow for methological pre-clinical studies.

Clinical proton treatment units were designed to operate at (clinical) dose rates of *gray (Gy) per minute*. Increasing the dose rate to *more than a hundred or even thousand gray per second* imposes a challenge on the air-filled planar ionization chambers commonly used as dose monitors. To deliver a preset amount of dose in the most accurate way, the beam is switched off after a certain amount of charge has been collected in a dose

monitor. If these detectors are irradiated at UHDR their charge collection efficiency decreases due to (volume) recombination effects (Palmans *et al* 2006). Without a correction the delivered dose would be systematically too large.

One of the most widely used methods to handle efficiency losses in gas-based detectors due to recombination effects (Mie 1904, Jaffé 1913) is the *Two-Voltage-Method (TVM)* (Boag and Currant 1980, Almond 1981, Weinhous and Meli 1984, Absorbed Dose Determination in External Beam Radiotherapy, IAEA 2001), on which the research of this paper is based. The *TVM* typically requires a measurement at nominal operating voltage and at a reduced voltage. From this, the collection efficiency 'is derived from the ratio of the voltages and the charges' (Liszka *et al* 2018).

The collection efficiency is however dose rate dependent (i.e. volume recombination increases with dose rate (Palmans *et al* 2006, Rossomme *et al* 2017)); if the dose rate varies, a re-measurement of the efficiency is required. Not only is the dose rate a function of the beam phase space (energy, size) but also of the beam intensity. The latter is subject to intentional variation for conventional versus UHDR studies, but also to random fluctuations in the accelerator output. To cope with such fluctuations, we propose a novel approach, which, in contrast to the standard *TVM* , uses two separate gas-based ionization detectors simultaneously at two different voltages and field strengths, in order to obtain an *in situ* recombination correction. This method yields a correction coefficient for *each* beam, independent of its energy or phase space.

The method we propose is fundamentally a generalization of the *TVM* by translation to two (geometrically) different detectors, which we call the *Two-Detectors-Two-Voltage-Method (2D2VM)*. We tested the method at the Gantry 1 beam line of the Paul Scherrer Institute, which has been recommissioned for UHDR (Nesteruk *et al* 2021). The hardware used are already existing gas-based ionization detectors mounted in the nozzle of Gantry 1. The objective of this work was to find appropriate operating conditions of the ionization chambers, as well as handling the fact that both of these devices are geometrically different and to ultimately verify the *2D2VM* . Since similar devices are present in other clinical machines, our method could be easily adapted to plane-parallel ionization chambers of other proton beam lines.

## 2. Methods

### 2.1. Beam delivery

A 250 MeV proton beam is delivered by the superconducting cyclotron COMET (Schippers *et al* 2007), where beam currents of up to 1 $\mu$A are available at the cyclotron exit. Afterwards a degrader is used to reduce the beam energy by driving graphite wedges into the beam, enabling beam energies between 230 MeV and 70 MeV for clinical or experimental applications. Through a variety of di- and quadrupole magnets, the beam is guided to the isocenter in the treatment room, see figure 1.

The use of a degrader is counter-productive for achieving UHDR due to multiple scattering and concomitant transmission losses in the energy selection system. In fact, the beam line transmission at 70 MeV is as low as 1‰ (van Goethem *et al* 2009). In order to achieve UHDR at the isocenter a special beam line setting was developed, focusing on high transmission (e.g. by fully driving the degrader wedges out of the beam) and narrow pencil beam shapes. Reported transmission (from COMET to isocenter) values at 250 MeV are better than 80%, allowing irradiation at peak dose rates of up to 9000 Gy $s^{-1}$ (Nesteruk *et al* 2021).

For the experiments described below, we have worked with a 250 MeV proton beam and local beam currents (in the nozzle, figure 1) of up to 700 nA, relating to a dose rate of up to 3600 Gy $s^{-1}$ (Gaussian beam profile average of interval >90% of profile peak) at 3.5 cm in water equivalent depth (Nesteruk *et al* 2021).

### 2.2. Dose measurement

Beam delivery on Gantry 1 is done in dose-driven mode: the beam stays on until a certain preset dose is reached, i.e. until a certain amount of charge has been collected in a dose monitor (plane-parallel ionization chamber, Monitor 1) in the Gantry nozzle (see figure 1, zoomed part). The delivered dose is measured by a second dose monitor (Monitor 2), also located in the nozzle. A more detailed layout of these detectors is given in figure 2. Both detectors are operated with air at atmospheric conditions.

At high dose rates, charge recombination effects begin to appear and lead to an over-dosage, if not corrected, due to a decrease in the collection efficiency a longer beam-on time is required in order for the preset charge to be met. For first biological experiments performed at Gantry 1, the severity of this effect was characterized by employing a Faraday cup as an absolute recombination-free dose detector (Nesteruk *et al* 2021, Winterhalter *et al* 2021); by increasing the dose rate (by increasing the beam current), a decrease of the charge collection efficiency is observed, see figure 3. We assume that the normalized (to low dose rates, i.e. absent recombination effects) ratio of the Monitor 1 charge to the Faraday cup charge adequately represents the charge collection efficiency.

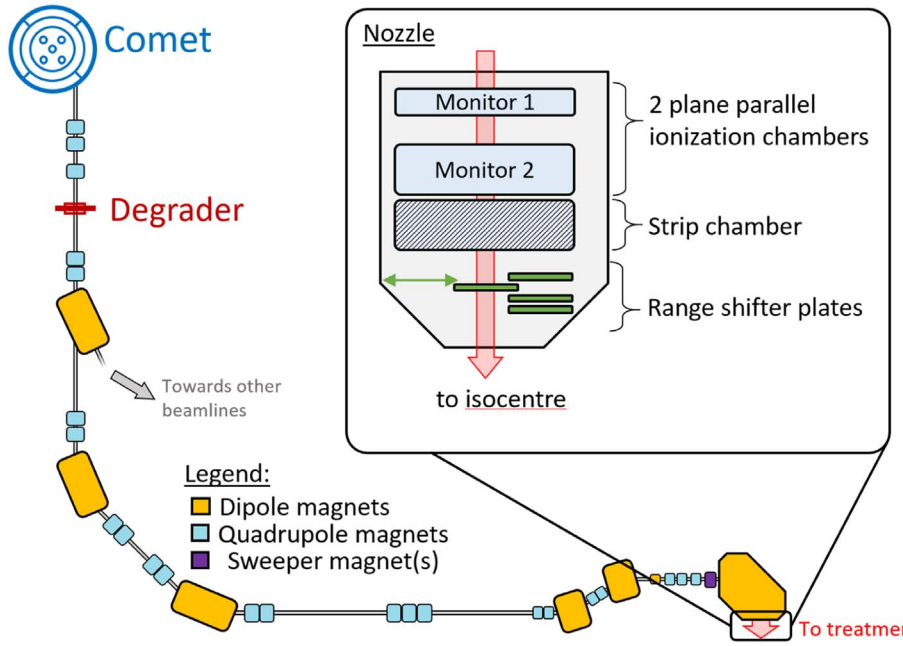


**Figure 1.** Layout of the beam line from the COMET cyclotron to the treatment area. The in-image zoomed part schematically represents the Gantry 1 nozzle, equipped with two plane-parallel ionization chambers for beam delivery control, a strip chamber for beam position measurement, and range shifter plates for beam energy modulation.

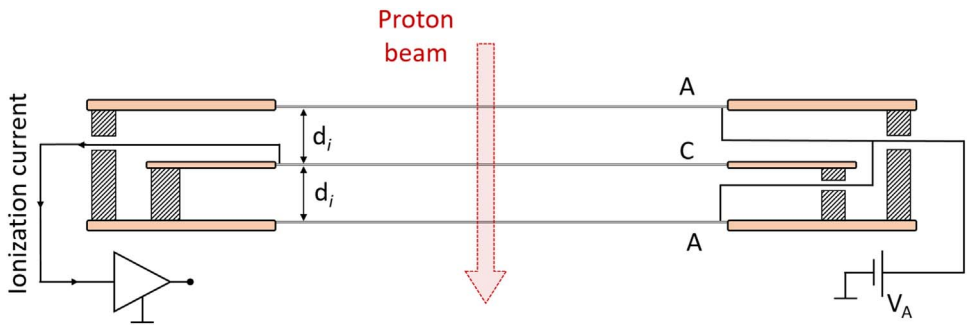


**Figure 2.** Layout of the plane parallel ionization chambers used in the nozzle. The gap sizes $d_i$ are 0.5 cm and 1 cm for Monitor 1 and 2, respectively; the nominal operating voltage during past clinical operations until late 2018 was at 2 kV on the anodes A.

In order to reproducibly irradiate samples at UHDR, the dose-rate dependent collection efficiency has to be considered when operating in dose-driven mode. An empirical correction, based on figure 3, is only meaningful for constant beam parameters (i.e. phase space and intensity) and detector settings. Daily variations in the order of a few percent in the beam line transmission are a common occurrence and eventually cause fluctuations in the delivered dose. An online measurement and -correction of the charge efficiency losses of (dose defining) monitors would improve the precision of the dose delivery at UHDR rates.

### 2.3. The generalised two-voltage-method: the two-detectors-two-voltage-method (2D2VM)

In the following, we check that the conditions for the *TVM* are fulfilled in our case, as well as introduce the generalization to two geometrically different detectors.

#### *2.3.1. Boundary conditions*

In the *TVM* , the collection efficiency $\eta_1$ (at voltage $U_1$) is determined by measuring the collected charges $Q_1$, $Q_2$ in a gas-based ionization chamber at two different voltages $U_1$, $U_2$ (Weinhous and Meli 1984):

$$\eta_1 = \left(\frac{U_1^2}{U_2^2} - \frac{Q_1}{Q_2}\right) \Big/ \left(\frac{U_1^2}{U_2^2} - 1\right). \tag{1}$$

This equation, however, is only valid under the following two circumstances:

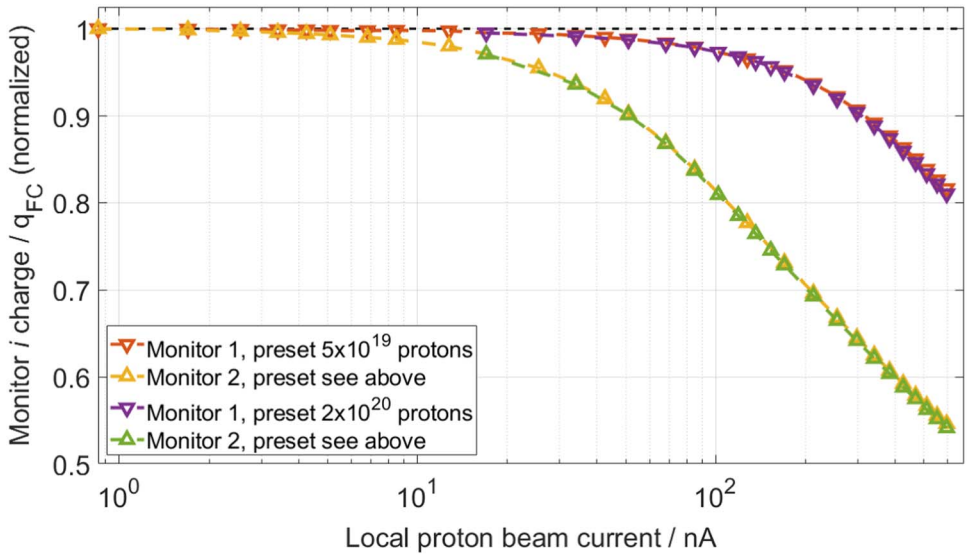


**Figure 3.** Collection efficiency (normalized, Monitor $i$ charge over Faraday cup charge $q_{FC}$) against (logarithmically) local beam current. The preset doses are given in number of protons. Here the two monitors (1: ▽, 2: △) are operated at (2 kV, 3 kV). Without correction for the charge losses, an over-dosage of up to 20% (dose defining: Monitor 1) would occur at high beam current. Since Monitor 1 and 2 have different air gap sizes and operating voltages, their collection efficiency is different.

**Continuous radiation.** The proton beam striking the detector must be continuous (Palmans *et al* 2006). This is the case, if the charge collection time is much longer than the beam pulse duration. For the two Monitors, the charge collection times are approx. 0.1 ms (Lin *et al* 2009), whereas the COMET beam pulses are 0.8 ns long with a period of 14 ns (Nesteruk *et al* 2021). Under these circumstances, the irradiation can be regarded as continuous. For cyclotrons, recombination correction has successfully been demonstrated experimentally in (Palmans *et al* 2006).

**Linear relation between $Q$ and $1/U^2$.** For continuous radiation, the collected charge $Q$ and the applied voltage $U$ are related via (Greening 1964):

$$Q_i = Q_0 - (\text{constant})(Q_i/U_i^2), \quad \text{and } Q_1 = \eta_1 \cdot Q_0, \tag{2}$$

where $Q_0$ is the collected charge at $\eta = 1$ and $i$ denotes a voltage setting. If the measurement of $1/Q_i \propto 1/U_i^2$ follows equation (2), the observed recombination effects are dominated by volume recombination (dose-rate dependent) and initial recombination (dependent on the ionization density along the track) can be neglected. The validity of this assumption has been tested in this work (see section 3.2 below).

Equation (1) is obtained by combining a set of equation (2) for $i = 1$ and $i = 2$, see appendix. An extensive analysis (Rossomme *et al* 2020) on the *TVM* emphasizes that the detector voltage has to be within this linear region. The validity of equation (2) is limited towards higher voltages due to charge multiplication effects in the detector (Rossomme *et al* 2021); this voltage is dose-rate and detector geometry dependent and is investigated for our detectors in section 3.1

In our generalized approach we intend to use the two plane parallel ionization chambers in the Gantry 1 nozzle to determine $\eta$ via equation (1), instead of using a single detector and repeatedly change the voltage. Since our monitors geometrically differ in gap size $d_{1,2}$, equation (1) has to be adapted for a two-detector-case via (Boag and Wilson 1952, Greening 1964):

$$U_i \rightarrow U_i/d_i^2, \tag{3}$$

where $i$ now denotes the different detectors. With this adaptation, equation (1) resembles the charge collection efficiency of Monitor 1. The application of equation (1) requires the (simultaneous) signals from both Monitor 1 and 2.

*2.3.2. Charge normalisation*

Signals from both detectors are first current-to-frequency (CFC) processed. Using these directly for a calculation of $\eta$ cannot be performed without some necessary corrections:

**Offset correction.** While not under irradiation, a stable offset rate (electronic noise as dark current) is observed on the monitors. By knowing the offset rate and the irradiation time $t$, the measured signal can be corrected:

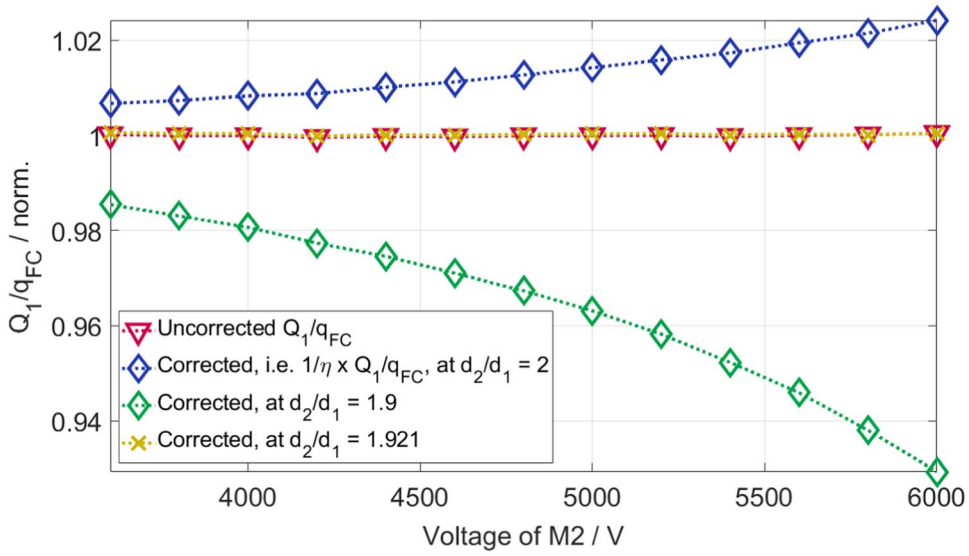


**Figure 4.** Plot of $Q_1$ over the (absolute) Faraday cup charge and application of the *2D2VM* at various gap ratios $d_2/d_1$. At low dose rates the collection efficiency is unity at the set detector voltages and the application of the *2D2VM* is without impact for the correct gap ratio ($\times$-marker), here shown as function of $U_2$. The $\Diamond$-marker curves show an application of the *2D2VM* with intentionally wrong gap ratios, resulting in $\eta \neq 1$.

$$M_i = M_{\text{measured},i} - (\text{Offset rate})_i \cdot t \tag{4}$$

At UHDR, typical delivery times are below 10 ms leading to an impact of the correction of less than 1%. Offset corrections are particularly important when working with low dose rates due to much longer delivery times.

**CFC conversion.** The collected charges in M1 and M2 are converted to counts through CFCs with an individual conversion factor for each detector. The frequency response behaves linearly to the input current, and a conversion factor was obtained from laboratory measurement with a current source. For the *2D2VM* , the measured counts are converted back to currents via the stated conversion factors.

**Different gap sizes.** Since the gap of M2 is twice that of M1, a larger signal in M2 is expected and observed. Consequently, this has to be corrected accordingly. By design, the gap ratio of M2 to M1 should be 10 mm/ 5 mm = 2, in reality, this is different through assembly.

The actual ratio can be obtained by estimating absent recombination effects at low dose rates. The amount of primary charges generated by a passing proton beam in the detectors behaves linearly with the traversed distance. Thus, the gap ratio equals the ratio of the (CFC converted and offset corrected) M1 and M2 charges, i.e. $d_2/d_1 = Q_2/Q_1$; for our case $d_2/d_1 = 1.921$.

This ratio has been checked by applying the *2D2VM* through equations (1) and (3) at absent recombination effects. With the determined gap ratio we expect $\eta = 1$, i.e. the *2D2VM* has no (and also should not have an) impact, see figure 4.

Eventually, by operating two plane parallel ionization chambers (M1 with gap $d_1$ and voltage $U_1$, M2 with $d_2$ and $U_2$) *simultaneously and consecutively* and by applying the aforementioned steps, we are able to do an *in situ* correction of the charge collection efficiency of the dose defining monitor (M1), i.e. the ratio of the corrected M1 charge over $q_{FC}$ (see figure 3) will become unity (within uncertainty) for local proton beam currents up to 700 nA.

## 3. Results

### 3.1. Voltage characteristics of the detectors

In order to correct recombination effects with the *2D2VM* , the onset and end of the linear region (equation (2)) has to be determined for both detectors; this was done by irradiating the detectors at UHDR (ca. 3600 Gy $s^{-1}$, corresponding to a local beam current of ca. 700 nA) to invoke (volume) recombination effects and scanning the detector operating voltage. The obtained data was normalized to Faraday cup measurements, 5.

To highlight the linear regions, or a deviation from it, fits were added to figures 5. The onset of the linear region for Monitor 1 is (visually) somewhere above 2 kV; from a conservative approach we chose 2.5 kV as the lower limit for the operating voltage. Due to the larger gap size of Monitor 2, the electrode voltage setting is higher, with the voltage being scanned from 4 to 6 kV and the operating value is greater than 5.6 kV. For both detectors, no charge multiplication effects were observed up to 3 kV in Monitor 1 and 6 kV in Monitor 2.

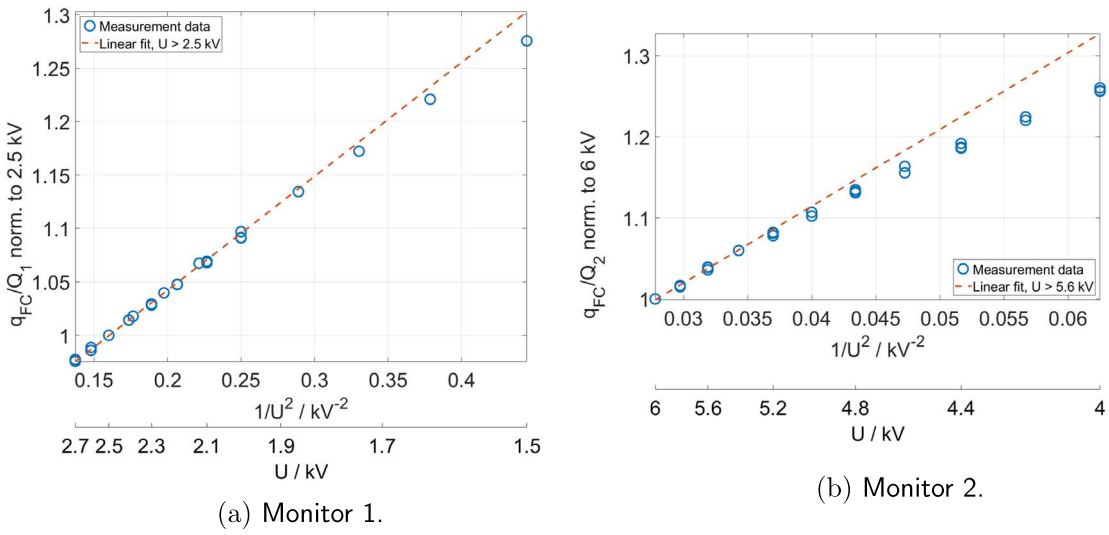


(a) Monitor 1. (b) Monitor 2.

**Figure 5.** Voltage scans of the two used detectors in the Gantry 1 nozzle at UHDR (i.e. local beam current of ca. 700 nA, corresponding to ca. 3600 Gy s$^{-1}$).

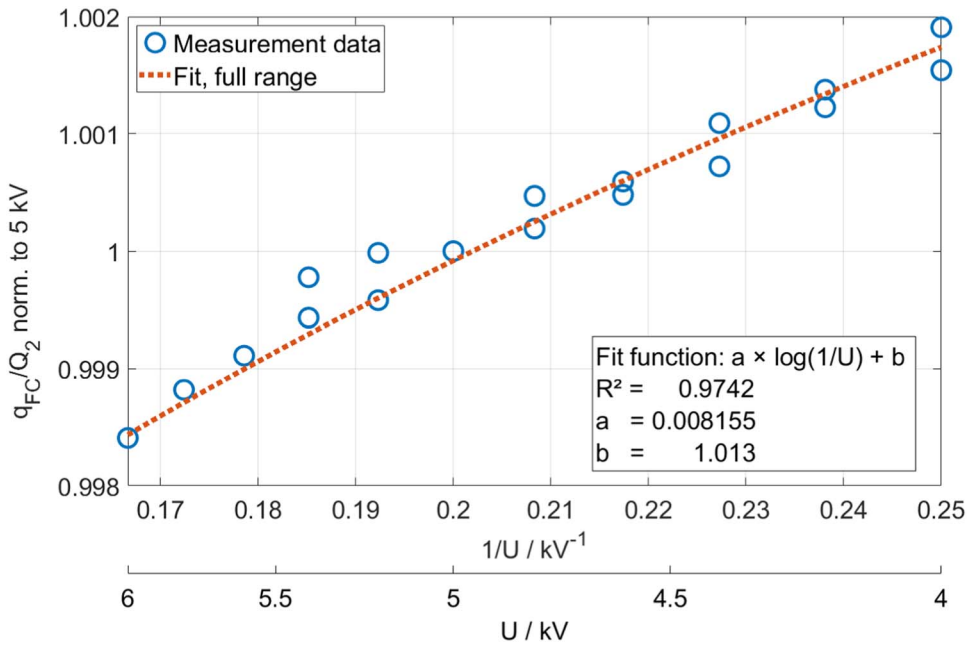


**Figure 6.** Normalized $1/Q$ against $1/U$ for Monitor 2, showing a logarithmic curve behavior, due to the dominating initial recombination effects. The dose rate is approximately 4.5 Gy s$^{-1}$, where volume recombination effects are absent.

### 3.2. Contribution of initial recombination

The application of equation (1) relies on absent initial recombination effects—in reality this is only valid by approximation. At high dose rates, volume recombination is dominant, whereas initial recombination becomes more significant at low dose rates. The latter can be determined by measurement of $1/Q_i$ against $1/U_i$ (here at approximately 4.5 Gy s$^{-1}$ at $\leqslant$0.85 nA local beam current). If the two quantities show a logarithmic relation, initial recombination is dominant (Rossomme *et al* 2017). On Monitor 1, we found this to be hardly noticeable as the variation of the collected charge between 2.7 kV and 2 kV was less than 0.5 ‰. For Monitor 2, in contrast, such a logarithmic dependence is clearly visible, figure 6.

The amount of initial recombination was computed with the `IonTracks` software (Christensen *et al* 2016), generalizing the Jaffé model (Jaffé 1913). For a 250 MeV proton beam, we find the following losses for both of the used detectors:

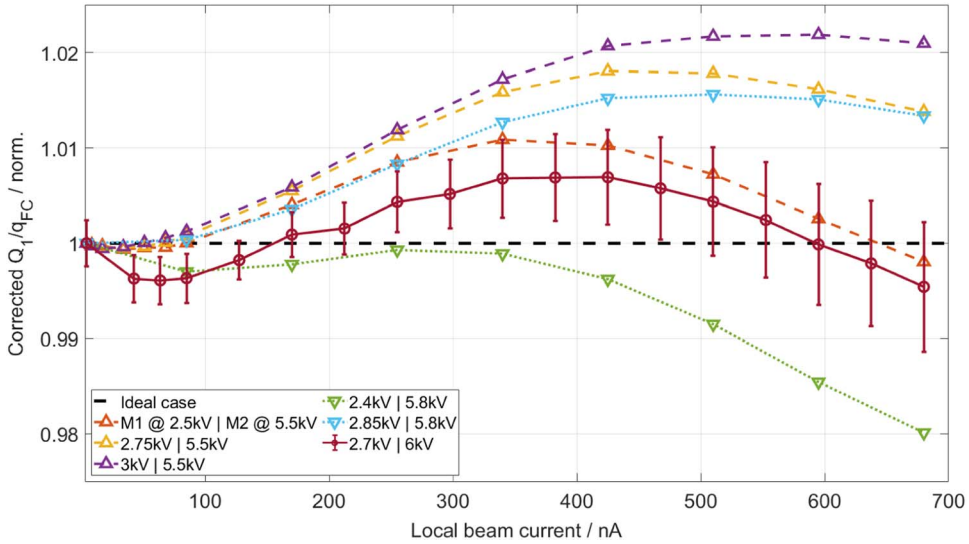


**Figure 7.** Normalized (to 4 nA local beam current) ratios of the corrected M1 charge to the Faraday cup charge for various combinations of detector voltages. For clarity reasons, uncertainty bars were omitted on all data sets except for the best approach (∘-markers). At 700 nA local beam current the uncorrected M1 collection efficiency is 89% for $U_1 = 2.4$ kV and 95% for 3 kV.

- **Monitor 1.** At 1.5 kV: $1 - \eta = 0.013\%$, at 6.5 kV: $1 - \eta = 0.004\%$,
- **Monitor 2.** At 1.5 kV: $1 - \eta = 0.074\%$, at 6.5 kV: $1 - \eta = 0.013\%$.

The different gap sizes of the detectors in our setup lead to a different contribution of initial recombination and eventually a systematic effect is expected when applying the *2D2VM* . However the results from the `IonTracks` simulation, indicate that initial recombination corrections <0.1% can be completely neglected for both ionization chambers used in this study for the detector voltage range (1.5–6.5) kV. The negligible amount of initial recombination in proton beams >70 MeV is in agreement with previous studies (Liszka *et al* 2018, Christensen *et al* 2020) separating the initial and general (volume) recombination components in proton beams.

### 3.3. Dose-rate dependency of the correction and voltage fine tuning

At ideal detector operating voltages, we expect to obtain dose rate independent (within their combined uncertainties) ratios of the corrected collected Monitor 1 charge $Q_1$ to the collected Faraday cup charge $q_{FC}$. Thus, $Q_1/q_{FC}$ (normalized to low dose rates), as depicted without correction in figure 3, is expected to become unity at all dose rates (i.e. local beam currents) after application of the *2D2VM* .

Figure 7 shows the impact of the *2D2VM* at various combinations of working voltages for M1 and M2 as a function of the local proton beam current. The data sets are split into △-markers ($U_1$ variation, $U_2$ fixed) and ▽-markers (vice versa). Each data set is normalized to a local beam current of 4 nA, where detector recombination effects are absent.

An approach towards the ideal case was made by fine-tuning the working voltages. We found the best approach to be at 2.7 kV (M1) and 6 kV (M2) (∘-markers), where 'best approach' refers to minimizing the residuals of the corrected ratio $Q_1/q_{FC}$ to the ideal case in an experimental, not in an analytical approach.

The uncertainties depicted in figure 7 are solely from the *2D2VM*-method and amount up to 5‰, relative to $Q_1/q_{FC}$. A detailed discussion of the uncertainties is given in the appendix. Relative uncertainties of the measured Faraday cup charge are 1‰ on the precision for repetitive successive measurements within a day (type A) and roughly the same for measurements separated by years (also type A) (Winterhalter *et al* 2021).

For our 'best-approach' detector settings, ratio $(Q_1/\eta)/q_{FC}$ does not show any significant (i.e. within 2 uncertainty intervals) dose rate dependence.

## 4. Discussion

As shown in figure 7, we found that different working voltages have a dominant effect for the *2D2VM* . Simply determining the onset of the linear region between the charge collected and the operating voltage (see section 3.1) is too coarse to simply apply the method. An improvement is made by fine-tuning the detector voltages, leading to a trade off between under-correcting at lower dose rates and over-correcting at higher dose

rates. An increase in $U_1$ reduces the amplitude across the dose rate range, but increases the impact at higher dose rates leading to an over-correction. An increase in $U_2$ has a rather small impact on the correction at low dose rates, where an increase in $U_2$ can lead to an under-correction at high dose rates. The curve shapes and the remaining deviation to an ideal correction are assumed to originate from an underlying effect related to the different gap sizes $d_{1,2}$. This however is not yet fully understood.

We found that our proposed generalisation of the *TVM* can be implemented relatively easily on existing hardware, provided that the operating conditions fulfill the assumptions of the method. The detectors must be in their linear region and dominated by volume recombination. Both assumptions are relatively easy to fulfill via a simple characterisation of the detectors in proton beams. We found that *2D2VM* provides a reliable correction for recombination effects for beam currents spanning over two orders of magnitude, with a residual deviation of less than a percent. The method proves especially useful in an environment where a variety of different beam settings are used, as in contrast to the *TVM* or absolute-detection based empirical correction curves, a (re-) determination for every new beam line and phase space setting that changes the dose rate, becomes obsolete.

Although there are recombination correction approaches that use multi-gap ionization chambers (Prieels 2009, Giordanengo and Palmans 2018), a principle somewhat similar to the presented method here, they require a calibration curve. In that sense, the *2D2VM* distances itself from such approaches, as no *a posteriori* calibration curve is required to initial charge collection efficiency measurements.

Our aim was to propose a method which can easily be implemented in clinical treatment units. This is certainly the case for systems using isochronous cyclotrons such as ours. The suitability of the *TVM* for high dose rate proton beams has however been questioned in the case of synchro-cyclotron beams (Darafsheh *et al* 2021). The suitability of the *2D2VM* in this context has not been tested, and the beam structure of an isochronous cyclotron and of synchro-cyclotrons is quite different to allow a simple extrapolation. Synchro-cyclotrons have typically millisecond repetition rates and microsecond pulse widths. If however the collection times of detectors are sufficiently long with respect to the pulse widths, our method should in principle also be applicable in this context.

## 5. Conclusions

We have successfully demonstrated that charge collection efficiency losses in a gas-based ionization chamber, caused by continuous irradiation with a proton beam at UHDR, can be corrected by translating the basic principles of the *TVM* to a second gas-based ionization chamber at different operation conditions, instead of changing the operating conditions on the primary detector. With the correction applied to the collected charge in our dose defining monitor, we were able to compensate the dose rate dependent volume recombination effects. This was further verified by comparison to an absolute measurement with a Faraday cup, where the ratio of the corrected monitor charge to the absolute Faraday cup charge showed no significant dose rate dependence (up to local beam currents of 700 nA, or respectively 3600 Gy $s^{-1}$). We have also demonstrated all steps of the implementation of the method on a former clinical unit, Gantry 1, thus showing an example which can be easily adapted to other facilities.

## Acknowledgments

We thank our collaborators at PSI (M Togno, B Rohrer, D Meer, T Lomax, J Christensen).

## Data availability statement

All data that support the findings of this study are included within the article (and any supplementary information files). Data will be available from 13 March 2023.

## Conflict of interest

The authors have no conflict to disclose.

# Appendix

### A.1. Uncertainty assessment of the *2D2VM*

Combining equation (1) and (3) yields the functional dependency of the collection efficiency $\eta$ and its parameters ($U_{1,2}$, $Q_{1,2}$, $d_{1,2}$). Before applying a Gaussian error propagation to this emerging function, we asses the uncertainty contributions of the single parameters below.

**Detector voltages** $U_1$, $U_2$. The detector voltages are set through potentiometers on the HV source. One full rotation of the rotary knob corresponds to 1 kV; a higher precision is enabled through tick marks in 100 V and 20 V steps. We assume that the voltage can be set to the desired value $\pm 5$ V. This uncertainty was determined by setting a variety of desired voltages and measuring the output (type A uncertainty, Gaussian distributed).

An additional contribution comes from the approach to compensate the initial recombination in Monitor 2 via fine tuning the voltage (see figure 7). As this was not an analytical approach, the voltage uncertainty is estimated as $\pm 50$ V (type B, Gaussian). In summary the total voltage uncertainty is $s_{U_{1,2}} = \sqrt{50^2 + 5^2}$ V.

**Collected charges** $Q_1$, $Q_2$. The collected charge in the detector is processed by a CFC which yields 'counts' as (rounded down) integers. Rounding down can be compensated by adding a half count to the measured number of counts, as well as to the offset rate. We consider the distribution of the measured counts to be rectangular within $\pm 0.5$ counts. This uncertainty is of type B. The irradiation time counter behaves similar, where 10 000 counts correspond to one second. The analogy above applies, i.e. half a count is added to the time counter, the uncertainty is $\pm 0.5$ counts (type B, rectangular distribution).

Eventually, the corrected counts are translated into a current by using the CFC calibration table. The data resembles a line through origin, i.e. a slope can be obtained from each tuple of input current and output frequency. As uncertainty we use the empirical standard deviation (type A) of the average slope:

$$\begin{aligned}\text{CFC M1: Slope} &= (9.9536 \pm 0.0201)\ \text{nC/count}\\ \text{CFC M2: Slope} &= (4.5032 \pm 0.0229)\ \text{nC/count.}\end{aligned}$$

Thus, from determining the charge $Q$ collected in the detector via:

$$Q_i = \frac{1}{\text{CFC Slope}_i}(M_i - (\text{Offset rate})_i \cdot t),$$

the uncertainty is (Gaussian error propagation):

$$s_{Q_i} = \frac{1}{\text{CFC Slope}}\sqrt{(Q_i \cdot s_{\text{Slope}})^2 + s_{\text{M}}^2 + (t \cdot s_{\text{M}})^2 + ((\text{Offset rate}_i) \cdot s_{\text{t}})^2}.$$

Since the gap size of M2 is roughly twice the gap size of M1, $Q_2$ needs to be divided by the gap ratio, adding up to $s_{Q_2}$.

**Gap ratio** $d_2/d_1$. To determine the uncertainty for the gap ratio, we apply Gaussian error propagation to the charge ratio $Q_2/Q_1$. The relative uncertainty of the gap ratio is approximately 3‰.

The relative difference between $d_2/d_1$ to $d_2/d_1|_{\pm 1\,\sigma}$ is roughly 3 per mil (type A, Gaussian).

Eventually, Gaussian error propagation can be applied to equation (1) and the above considerations to obtain an uncertainty for $\eta$. We obtain relative uncertainties for $\eta$ of 2.5‰ towards low dose rates (i.e. at local beam currents <80 nA), and 6.8‰ towards high dose rates (i.e. at local beam currents >500 nA)

### A.2. Algebraic derivation of the charge collection efficiency based on the collected charge

To derive equation (1), we start with equation (2) and calculate $Q_1$ and $Q_2$, i.e. $i = 1$ and $i = 2$:

$$Q_1 = Q_0 - (\text{constant})(Q_1/U_1^2) \tag{5}$$

$$Q_2 = Q_0 - (\text{constant})(Q_2/U_2^2) \tag{6}$$

equations (5) and (6) are then separately solved for 'constant':

$$\text{constant} = (Q_0 - Q_1) \cdot \frac{U_1^2}{Q_1} \tag{7}$$

$$\text{constant} = (Q_0 - Q_2) \cdot \frac{U_2^2}{Q_2} \tag{8}$$

We equate (7) and (8), and simplify:

$$(Q_0 - Q_1) \cdot \frac{U_1^2}{Q_1} = (Q_0 - Q_2) \cdot \frac{U_2^2}{Q_2}$$
$$\left(\frac{Q_0}{Q_1} - \frac{Q_1}{Q_1}\right)U_1^2 = \left(\frac{Q_0}{Q_2} - \frac{Q_2}{Q_2}\right)U_2^2 \tag{9}$$

We use $Q_1 = \eta_1 \cdot Q_0 \rightarrow Q_0 = Q_1/\eta_1$ on equation (9) to get rid of $Q_0$:

$$\left(\frac{1}{\eta_1} - 1\right)U_1^2 = \left(\frac{Q_1}{Q_2}\frac{1}{\eta_1} - 1\right)U_2^2$$

We further simplify and solve for $\eta_1$:

$$\frac{U_1^2}{\eta_1} - U_1^2 = \frac{Q_1}{Q_2}\frac{1}{\eta_1}U_2^2 - U_2^2$$
$$\frac{1}{\eta_1}\left(U_1^2 - \frac{Q_1}{Q_2}U_2^2\right) = U_1^2 - U_2^2$$
$$\eta_1 = \left(U_1^2 - \frac{Q_1}{Q_2}U_2^2\right)/U_1^2 - U_2^2$$
$$\eta_1 = U_2^2\left(\frac{U_1^2}{U_2^2} - \frac{Q_1}{Q_2}\right)/U_2^2\left(\frac{U_1^2}{U_2^2} - 1\right). \tag{10}$$

Eventually equation (10) resembles the charge collection efficiency as given in equation (1).

## References


Almond P R 1981 Use of a Victoreen 500 electrometer to determine ionization chamber collection efficiencies *Med. Phys.* **8** 901–4

Beyreuther E, Brand M, Hans S, Hideghéty K, Karsch L, Leßmann E, Schürer M, Szabó E R and Pawelke J 2019 Feasibility of proton FLASH effect tested by zebrafish embryo irradiation *Radiother. Oncol.* **139** 46–50

Boag J W, Grau C, Overgaard C, Andersen C E, Kanouta E and Currant J 1980 Current collection and ionic recombination in small cylindrical ionization chambers exposed to pulsed radiation *Br. J. Radiol.* **53** 471–8

Boag J W and Wilson T 1952 The saturation curve at high ionization intensity *Br. J. Appl. Phys.* **3** 222–9

Christensen J B, Almhagen E, Stolarczyk L, Liszka M, Hernandez G G, Bassler N, Nørrevang O and Vestergaard A 2020 Mapping initial and general recombination in scanning proton pencil beams *Phys. Med. Biol.* **65** 115003

Christensen J B, Tölli H and Bassler N 2016 A general algorithm for calculation of recombination losses in ionization chambers exposed to ion beams *Med. Phys.* **43** 5484–92

Cunningham S *et al* 2021 FLASH proton pencil beam scanning irradiation minimizes radiation-induced leg contracture and skin toxicity in mice *Cancers* **13** 1012–27

Darafsheh A, Hao Y, Zhao X, Zwart T, Wagner M, Evans T, Reynoso F and Zhao T 2021 Spread-out Bragg peak proton FLASH irradiation using a clinical synchrocyclotron: Proof of concept and ion chamber characterization *Med. Phys.* **48** 4472–84

Diffenderfer E S *et al* 2020 Design, implementation, and *in vivo* validation of a novel proton FLASH radiation therapy system *Int. J. Radiat. Oncol. Biol. Phys.* **106** 440–8

Favaudon V *et al* 2014 Ultrahigh dose-rate FLASH irradiation increases the differential response between normal and tumor tissue in mice *Sci. Transl. Med.* **6** 245ra93

Giordanengo S and Palmans H 2018 Dose detectors, sensors, and their applications *Med. Phys.* **45** e1051–72

Greening J R 1964 Saturation characteristics of parallel-plate ionization chambers *Phys. Med. Biol.* **9** 143–54

IAEA 2001 *Absorbed Dose Determination in External Beam Radiotherapy* 398 International Atomic Energy Agency, Vienna

Jaffé G 1913 Zur theorie der ionisation in kolonnen *Ann. Phys.* **347** 303–44

Lin S, Boehringer T, Coray A, Grossmann M and Pedroni E 2009 More than 10 years experience of beam monitoring with the Gantry 1 spot scanning proton therapy facility at PSI *Med. Phys.* **36** 5331–40

Liszka M, Stolarczyk L, Kłodowska M, Kozera A, Krzempek D, Mojżeszek N, Pedracka A, Waligórski M P R and Olko P 2018 Ion recombination and polarity correction factors for a plane-parallel ionization chamber in a proton scanning beam *Med. Phys.* **45** 391–401

Mie G 1904 Der elektrische Strom in ionisierter Luft in einem ebenen Kondensator *Ann. Phys.* **318** 857–89

Nesteruk K P, Togno M, Grossmann M, Lomax A J, Weber D C, Schippers J M, Safai S, Meer D and Psoroulas S 2021 Commissioning of a clinical pencil beam scanning proton therapy unit for ultra-high dose rates (FLASH) *Med. Phys.* **48** 4017–26

Palmans H, Thomas R and Kacperek A 2006 Ion recombination correction in the Clatterbridge Centre of Oncology clinical proton beam *Phys. Med. Biol.* **51** 903–17

Prieels D 2009 Device and method for measuring an energy particle beam *WIPO (PCT)* WO2011009953A1

Rossomme S, Delor A, Lorentini S, Vidal M, Brons S, Jäkel O, Cirrone G A P, Vynckier S and Palmans H 2020 Three-voltage linear method to determine ion recombination in proton and light-ion beams *Phys. Med. Biol.* **65** 045015

Rossomme S, Lorentini S, Vynckier S, Delor A, Vidal M, Lourenço A and Palmans H 2021 Correction of the measured current of a small-gap plane-parallel ionization chamber in proton beams in the presence of charge multiplication *Z. für Med. Phys.* **31** 192–202

Rossomme S *et al* 2017 Ion recombination correction factor in scanned light-ion beams for absolute dose measurement using plane-parallel ionisation chambers *Phys. Med. Biol.* **62** 5365–82

Schippers J, Dölling R, Duppich J, Goitein G, Jermann M, Mezger A, Pedroni E, Reist H and Vrankovic V 2007 The SC cyclotron and beam lines of PSI's new protontherapy facility PROSCAN *Nucl. Instrum. Methods Phys. Res.* B **261** 773–6

Singers Sørensen B, Krzysztof Sitarz M, Ankjærgaard C, Johansen J and Poulsen P 2022 *In vivo* validation and tissue sparing factor for acute damage of pencil beam scanning proton FLASH *Radiother. Oncol.* **167** 109–15

van Goethem M J, van der Meer R, Reist H W and Schippers J M 2009 Geant4 simulations of proton beam transport through a carbon or beryllium degrader and following a beam line *Phys. Med. Biol.* **54** 5831–46

Vozenin M-C *et al* 2019 The advantage of FLASH radiotherapy confirmed in mini-pig and cat-cancer patients *Clin. Cancer Res.* **25** 35–42

Weinhous M S and Meli J A 1984 Determining Pion, the correction factor for recombination losses in an ionization chamber *Med. Phys.* **11** 846–9

Wilson J D, Hammond E M, Higgins G S and Petersson K 2019 Ultra-High Dose Rate (FLASH) radiotherapy: silver bullet or fool's gold? *Frontiers Oncol.* **9** 1–12

Winterhalter C, Togno M, Nesteruk K P, Emert F, Psoroulas S, Vidal M, Meer D, Weber D C, Lomax A and Safai S 2021 Faraday cup for commissioning and quality assurance for proton pencil beam scanning beams at conventional and ultra-high dose rates *Phys. Medi. Biol.* **66** 124001